C. R. Chimie 20 (2017) 40–46

Contents lists available at ScienceDirect

Comptes Rendus Chimie

www.sciencedirect.com

Full paper/Mémoire

Promotion of lanthanum-supported cobalt-based catalysts for the Fischer–Tropsch reaction

Promotion par le lanthane des catalyseurs à base de cobalt pour la réaction Fischer–Tropsch

Cathy Brabant [a, b], Andrei Khodakov [a, b], Anne Griboval-Constant [a, b, *]

[a] *Université Lille Nord de France, 59000 Lille, France*
[b] *CNRS UMR8181, Unité de Catalyse et Chimie du Solide – UCCS, 59652 Villeneuve-d'Ascq, France*

ARTICLE INFO

Article history:
Received 3 September 2015
Accepted 4 February 2016
Available online 21 March 2016

Keywords:
Fischer–Tropsch synthesis
Cobalt catalyst
Lanthanum

ABSTRACT

This paper focuses on the effect of the La/Co ratio on the structure of alumina cobalt supported catalysts for Fischer–Tropsch synthesis. Catalysts are prepared by wetness impregnation of alumina followed by calcination in air. The catalysts contain 10 wt% of cobalt and between 0 and 20 wt% of La (0, 5, 10, 15, 20). The catalysts were activated by reduction in hydrogen at 673 K and the catalytic performance was evaluated in a fixed bed reactor at 20 bar and 493 K. A wide range of techniques (BET, XRD, TPR, and XPS) were used for catalyst characterization at each preparation step and showed strong impact of the La/Co ratio on the structure, reducibility of supported cobalt phases. It was shown that 10 wt% of lanthanum allows reducing cobalt aluminate and improving catalytic performances.

Mots-clés :
Synthèse Fischer–Tropsch
Catalyseurs à base de Co
Lanthane

RÉSUMÉ

Ce document présente l'effet du rapport La/Co sur la structure des catalyseurs à base de cobalt supporté sur alumine pour la synthèse Fischer–Tropsch. Les catalyseurs sont préparés par imprégnation à sec de l'alumine suivie par une calcination sous air. Les catalyseurs contiennent 10% en masse de cobalt et entre 0 et 20% de La (0, 5, 10, 15, 20). Les catalyseurs ont été activés par réduction sous hydrogène à 673 K et les performances catalytiques ont été évaluées dans le réacteur à lit fixe à 20 bar et 493 K. Différentes techniques (BET, XRD, TPR, XPS) ont été utilisées pour la caractérisation des catalyseurs à chaque étape de la préparation, et les résultats ont montré un impact fort du rapport La/Co sur la structure et la réductibilité des phases. Une teneur de 10% de lanthane permet de réduire la formation d'aluminate de cobalt et d'améliorer les performances catalytiques.

* Corresponding author. Unité de Catalyse et de Chimie du Solide, Université de Lille, Bât. C3, Cité Scientifique, 59655 Villeneuve-d'Ascq, France.
E-mail address: anne.griboval@univ-lille1.fr (A. Griboval-Constant).

http://dx.doi.org/10.1016/j.crci.2016.02.006

1. Introduction

Fischer–Tropsch (FT) synthesis is an essential part of the GTL, CTL and BTL technologies which manufacture valuable hydrocarbons free of sulfur, nitrogen and aromatics from natural gas, coal or biomass. The current interest in FT synthesis has been largely driven by growing demand for clean fuels and rational utilization of the different resources [1–4].

The reaction produces a wide range of hydrocarbons from synthesis gas (mixture of carbon monoxide and hydrogen) used with a H_2/CO ratio close to 2. Cobalt catalysts supported by refractory oxides are preferentially used for the production of middle distillates and waxes [4–7]. These catalysts are typically prepared by impregnation with cobalt nitrate followed by oxidative or/and reductive pretreatments. High cobalt dispersion, good reducibility and catalyst stability are key parameters to attain high and enduring yields of hydrocarbons. Alumina-supported cobalt catalysts are generally preferred for FT synthesis due to their high activity, high selectivity to linear paraffins and low water gas shift activity [4]. Moreover alumina has the advantage of having a high surface area, porosity, thermal stability and good mechanical properties and then has been especially convenient for the design of cobalt FT catalysts for fixed-bed reactors. On the other hand, the metal-support interaction in alumina-supported catalysts can also result in a mixed oxide (cobalt aluminate) [8,9], which should be avoided, since it does not catalyze FT synthesis. Minimization of the concentration of barely reducible cobalt aluminate and maximization of cobalt metal dispersion would therefore result in a better catalytic performance. The use of different dopants was reported in the literature. Indeed the performance of cobalt catalysts can be enhanced by using promotion with noble metals (Pt, Rh, and Re) which allows increasing cobalt reducibility [4]. Previous reports [10,11] have shown that promotion with lanthanum could improve the performance of cobalt FT catalysts. Moreover Barrault et al. [12] reported the formation of new active sites for La promoted Co/C catalysts, which induce an increase in the specific activity in CO hydrogenation. Haddad et al. [13] studied a La-promoted Co/SiO_2 catalyst system using steady-state isotopic transient kinetic analysis (SSITKA) and found that the addition of La^{3+} did not alter the nature of the active sites. However, La^{3+} promotion increases the activity by increasing the concentration of intermediates for Fischer–Tropsch synthesis. According to Ernst et al., the use of La or Ce in the preparation of cobalt catalyst increases the formation of methane and light hydrocarbons and decreases the production of heavy hydrocarbons. This effect has been attributed to the reduction of cobalt crystallites sizes [14]. The increase of methane formation has been also observed on Co/TiO_2 catalysts [15]. On the other hand, Cai et al. reported a best reducibility and a low methane formation of cobalt promoted catalyst when La_2O_3 is used [16]. Thus at present the mechanism of the modification of the catalyst structure by using a lanthanum promoter and its influence on the catalytic performance remain, however, rather erratic.

This paper focuses on the effect of the La/Co ratio on the structure of alumina cobalt supported catalysts and their catalytic performance in FT synthesis. Catalysts are prepared by wetness impregnation of Puralox alumina followed by calcination in air. Typically, the catalysts contain 10 wt% of cobalt and between 0 and 20 wt% of La (0, 5, 10, 15, 20). Cobalt was introduced on the lanthanum calcined catalyst. A co-impregnated catalyst with 10 wt% of Co and 10 wt% of La was used for comparison. The catalysts were activated by reduction in hydrogen at 673 K and the catalytic performance was evaluated in a fixed bed reactor. At different stages of the preparation (calcination and reduction), the catalysts were characterized by nitrogen adsorption, X-ray diffraction (XRD), X-ray photoelectron spectroscopy (XPS), and temperature programmed reduction (TPR). The characterization results are discussed together with the results of catalytic evaluation in a fixed bed reactor.

2. Experimental

Catalysts were synthesized via incipient wetness impregnation using aqueous solutions of cobalt nitrate and lanthanum nitrate. Alumina (Puralox SCCA 5/170, Sasol, pore volume = 0.43 $cm^3\,g^{-1}$, average pore diameter = 9 nm) was used as the catalytic support. The catalysts were prepared in two consecutive impregnations separated by drying and calcination under air flow. At first lanthanum was introduced on the support followed by cobalt introduction on the lanthanum calcined catalyst. The cobalt content in the catalysts is 10 wt% and the lanthanum content varies between 0 and 20 wt%. A co-impregnation catalyst with 10 wt% of Co and 10 wt% of La was synthesized for comparison. The impregnated catalysts were dried 10 h at 373 K and calcined 5 h at 673 K in a flow of air (heating ramp 1 °C/min). The modes of lanthanum and cobalt introduction in catalyst synthesis is described in Fig. 1. The calcined catalysts are labeled as ***x*La/Al_2O_3** where ***x*** indicates the lanthanum content (0, 5, 10, 15, 20 wt%) and **10Co*x*La/Al_2O_3**. The co-impregnated catalyst is denoted as **co-10Co10La/Al_2O_3**.

The solids were characterized by several characterization techniques. The surface areas were measured by a standard BET procedure using nitrogen adsorption at

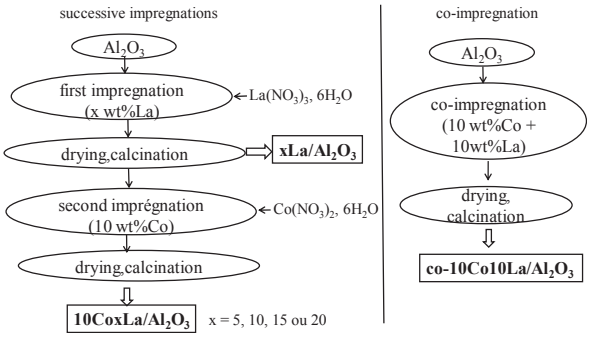

Fig. 1. Modes of lanthanum and cobalt introduction in catalyst synthesis and nomenclature.

−196 °C on a Micromeritics ASAP 2010 setup. X-ray powder diffraction experiments were conducted using a Brucker AXS D8 diffractometer using the Cu Kα radiation for crystalline phase detection. The average crystallite size of Co_3O_4 was calculated using 511 ($2\theta = 59.5°$) diffraction lines according to the Scherrer equation [17]. The reducibility of the catalysts was studied by temperature programmed reduction (TPR). The TPR was carried out by using an AutoChem II 2920 apparatus from Micromeritics in 5 vol.% H_2/Ar stream (3.6 NL h^{-1} g^{-1}) using 0.2 g of the sample. The temperature was risen from room temperature to 1273 K at a rate of 5 K/min. Surface analyses were performed using a VG ESCALAB 220XL X-ray photoelectron spectrometer (XPS). The $Al_{k\alpha}$ non-monochromatized line (1486.6 eV) was used for excitation with a 300 W-applied power. The analyzer was operated in a constant pass energy mode (E_{pass} = 40 eV). Binding energies were referenced to the Al_{2p} core level (74.6 eV) of the support. The vacuum level during the experiment was better than 10^{-7} Pa. The powdered catalyst was pressed into a thin pellet onto a steel block. The reproducibility was ±0.2 eV for La 3d and Co 2p binding energy.

Carbon monoxide hydrogenation was carried out in a fixed bed stainless steel tubular microreactor operating at 20 bar. The catalyst loading was 200 mg.

Prior to the catalytic test, all the samples were activated in a flow of pure hydrogen at atmospheric pressure during 10 h at 673 K with at GHSV = 2 NL h^{-1} g^{-1}. During the reduction, the temperature ramp was 3 K/min. After the reduction, the catalysts were cooled down to 433 K and a flow of premixed synthesis gas at a molar ratio $H_2/CO = 2$ was gradually introduced through the catalysts. Then, the temperature was slowly increased to 493 K. Gaseous reaction products were analyzed on-line by gas chromatography. Analysis of H_2, CO, CO_2 and CH_4 was performed using a packed CTR-1 column and a thermal conductivity detector. Hydrocarbons (C_1–C_9) were separated in a capillary Poraplot Q column and analyzed with a flame-ionization detector. The carbon monoxide contained 5% of nitrogen, which was used as an internal standard for calculating carbon monoxide conversion. The hydrocarbon selectivities were calculated on a carbon basis.

3. Results and discussion

3.1. x*La/Al$_2$O$_3$ calcined samples*

The nitrogen adsorption–desorption isotherms and pore size distribution curves calculated using the BJH method are shown in Fig. 2. The isotherms exhibit a hysteresis loop typical for capillary condensation in the mesoporous alumina support. Fig. 2 and Table 1 show that lanthanum introduction on alumina leads to a decrease both in the specific surface area and in the total pore volume. This effect was especially pronounced for the catalysts prepared with more than 15 wt% of lanthanum. The decrease in the BET surface area and pore volume is likely to be principally due to plugging support pores by lanthanum species and the effect of support "dilution" with lanthanum. The plugging makes the pores inaccessible for nitrogen adsorption. Fig. 2 shows that the introduction of

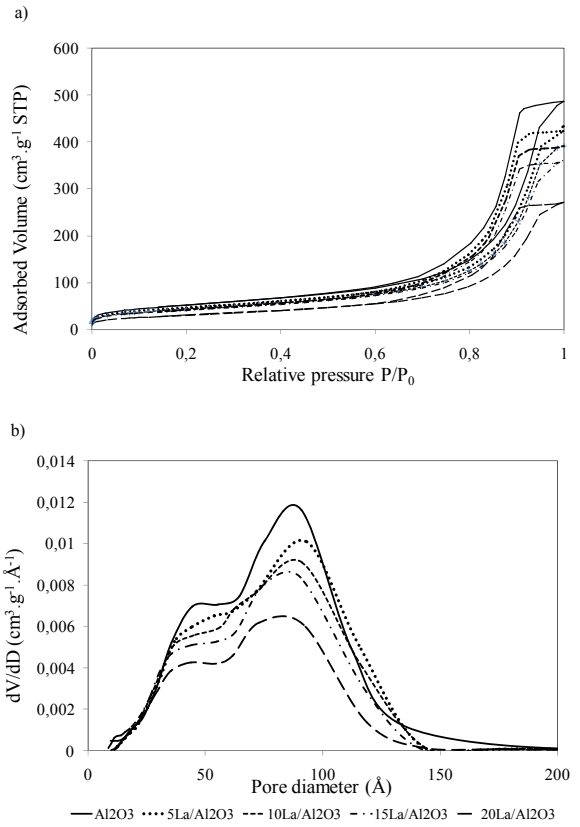

Fig. 2. a) Isotherms of nitrogen adsorption desorption and b) BJH pore size distribution curves on the xLa/Al_2O_3 calcined catalysts.

lanthanum does not modify the shape of pore size distribution curves. However, the presence of lanthanum results in a small decrease of the average pore diameter for 15La/Al_2O_3 and 20La/Al_2O_3 catalysts in agreement with the more pronounced decrease of the surface area observed for these solids.

The chemical state of the elements and the surface composition of the calcined samples were determined by X-ray photoelectron spectroscopy. La 3d XPS spectra of the catalysts and the binding energies of La $3d_{5/2}$ are presented in Fig. 3 and Table 2 respectively. The shape of the spectra is similar whatever the catalysts studied and is characteristic of La^{3+} [18]. The results show that the position of XPS La 3d peak shifts to the region of lower binding energies when the percent of lanthanum introduced increases (Table 2). This observation is in agreement with a higher interaction

Table 1
Characterization of lanthanum calcined catalysts.

Catalyst	BET surface area (m^2 g^{-1})	Total pore volume (cm^3 g^{-1})	Average pore diameter (nm)
Al_2O_3	187	0.43	9.1
5La/Al_2O_3	170	0.39	9.2
10La/Al_2O_3	158	0.36	8.9
15La/Al_2O_3	151	0.35	8.4
20La/Al_2O_3	114	0.26	8.2

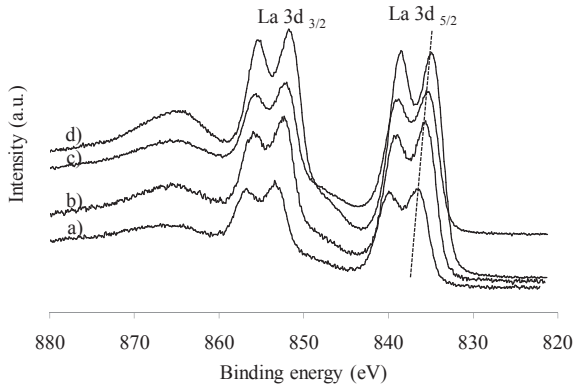

Fig. 3. La3d XPS spectra of lanthanum calcined catalysts: a) $5La/Al_2O_3$, b) $10La/Al_2O_3$, c) $15La/Al_2O_3$, and d) $20La/Al_2O_3$.

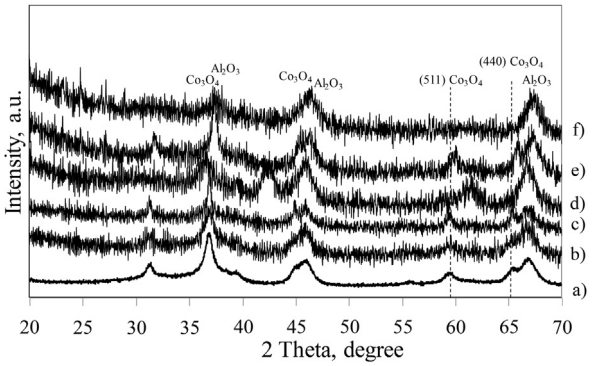

Fig. 4. XRD patterns of calcined catalysts: a) $10Co/Al_2O_3$, b) $10Co5La/Al_2O_3$, c) $10Co10La/Al_2O_3$, d) co-$10Co10La/Al_2O_3$, e) $10Co15La/Al_2O_3$, and f) $10Co20La/Al_2O_3$.

between lanthanum and the support which is obtained when the percent of lanthanum is lower, as described in the literature [11]. The La/Al atomic ratios are summarized in Table 2, calculated from the intensities of the La $3d_{5/2}$ signal, with atomic sensitivity factors given by Wagner et al. [19]. It can be noted that the La/Al atomic ratios are higher than the expected theoretical values derived from the bulk composition. Moreover, while calculating the $(La/Al)_{XPS}/(La/Al)_{bulk}$ ratio we observed that the lanthanum enrichment of the surface is more important when the percent of lanthanum is higher (20 wt% of La). All these observations are in agreement with the coverage of the support with layers of lanthanum. A high value of the $(La/Al)_{XPS}/(La/Al)_{bulk}$ ratio is obtained for the catalyst prepared with 20 wt% of lanthanum. This observation can be explained by the fact that due to the high coverage of the alumina surface, the reduction of Al signals is more pronounced.

3.2. Cobalt-lanthanum catalysts

3.2.1. Characterization

The XRD patterns of the calcined catalysts (Fig. 4) represent a combination of peaks attributed to γ-Al_2O_3 and Co_3O_4 crystalline phases. The particle size values for cobalt oxide crystallites in the catalysts calculated using the Scherrer equation are presented in Table 3. The size of Co_3O_4 crystallites was about 11 nm in $10Co/Al_2O_3$ as expected. Moreover it was shown that the sizes of cobalt oxide particles in supported catalysts prepared via aqueous impregnation with cobalt nitrate were principally affected by the support pore sizes [4]. For 10 and 15 wt% of lanthanum, the crystallite sizes of Co_3O_4 are quite similar. Previous reports [4,20] showed the reducibility of cobalt particles supported by alumina depended mostly on their sizes. Smaller cobalt particles are usually more difficult to reduce than the larger ones. It was reported that as the sizes of cobalt particles reach 8–10 nm, the cobalt oxide particles could be reduced more easily. Thus for $10Co10La/Al_2O_3$ and $10Co15La/Al_2O_3$ the Co_3O_4 crystallite sizes obtained are near the optimum value known to induce high reducibility of cobalt particles and good catalytic performances. However, for the $10Co5La/Al_2O_3$ catalyst the Co_3O_4 average crystallite size is smaller than the optimum size due to higher dispersion. Furthermore only very broad low intensity XRD peaks are observed for the $10Co20La/Al_2O_3$ catalyst, indicating low concentrations of the cobalt oxide crystalline phase. This can suggest a high dispersion of cobalt on the support or the high concentration of hardly reducible amorphous cobalt aluminate. The XRD pattern obtained for the catalyst prepared by co-impregnation of cobalt and lanthanum is different (Fig. 4d). We observed an intense peak at 42° which is not present on the other patterns. This peak can be attributed to the formation of a perovskite as $LaCoO_3$ (fiche JCPDS 01-084-0848), in agreement with the Co/La ratio equal to 1 in the impregnating solution.

Surface analyses of the cobalt-lanthanum calcined samples have been performed by XPS spectroscopy. The similar shape of the La 3d XPS spectra of the catalysts and the binding energies of La $3d_{5/2}$ (Table 4) are characteristics of La^{3+}. The shift of the position of the XPS La 3d peak to the region of lower binding energies, when the percent of

Table 2
XPS results for xLa/Al_2O_3 calcined supported catalysts.

Catalyst	B.E. (La $3d_{5/2}$) (eV)	La/Al Atomic ratio from XPS	La/Al Atomic ratio bulk	XPS/bulk
$5La/Al_2O_3$	836.0	0.03	0.02	1.7
$10La/Al_2O_3$	835.5	0.10	0.04	2.7
$15La/Al_2O_3$	835.4	0.14	0.06	2.4
$20La/Al_2O_3$	835.2	0.34	0.08	4.5

Table 3
XRD results for $10CoxLa/Al_2O_3$ calcined supported catalysts.

Catalyst	Size of Co_3O_4 crystallites by XRD (nm)
$10Co/Al_2O_3$	11
$10Co5La/Al_2O_3$	6
$10Co10La/Al_2O_3$	9
co-$10Co10La/Al_2O_3$	n.d.
$10Co15La/Al_2O_3$	12
$10Co20La/Al_2O_3$	n.d.

lanthanum introduced increases, observed previously for the lanthanum catalyst is not observed for the La–Co catalyst. This observation could be related to the modification of lanthanum dispersion by cobalt deposition. It can be noted that the La/Al atomic ratios are higher than the expected theoretical values derived from the bulk composition as for the lanthanum catalyst. Moreover, while calculating the $(La/Al)_{XPS}/(La/Al)_{bulk}$ ratio we observed that the lanthanum enrichment of the surface is more important after cobalt deposition (comparing Tables 1 and 2). The presence of carbon has been evidenced and the C/Al ratio increases with the lanthanum content in agreement with higher concentrations of carbonate species.

The Co2p XPS spectra (Fig. 5, Table 4) are indicative of the presence of Co_3O_4 which was identified by the binding energies (780.1 eV), peak shape, spin-orbital splitting of 15.2 eV and absence of intense satellite structures [21–24]. This observation is consistent with XRD data. However a shift of the Co $2p_{3/2}$ peak to the region of higher binding energies is observed for 15 wt% and 20 wt% of lanthanum. Those values and the broader signal are in agreement with the presence of Co^{2+} ions at the surface. In a more quantitative manner, cobalt dispersion in the calcined catalysts was evaluated from the n_{Co}/n_{Al} ratios determined by XPS compared with the theoretical atomic ratio corresponding to the monolayer coverage of the support by cobalt (Table 4). We observed that the cobalt is well-dispersed as a monolayer when lanthanum is deposited up to 10 wt%. The dispersion is better than the ones observed for the cobalt monometallic catalyst. For 15 wt% and 20 wt% of La, the Co/Al atomic ratios are higher than the expected theoretical values derived from the bulk composition. This can be resulted from the agglomeration of cobalt. However we cannot exclude that this observation results from the high reduction of Al signal due to the coverage of the support with a high La content.

The reducibility of the cobalt–lanthanum catalysts was studied by the temperature program reduction. The TPR profiles of the $10Co/Al_2O_3$ catalyst (Fig. 6a) exhibit three groups of hydrogen consumption peaks: low, medium and high temperature peaks. In agreement with previous reports [25–27], the low temperature peaks between room temperature and 603 K were mainly attributed to the reduction of Co_3O_4 to CoO. The small shoulder at 453 K seems to be related to the decomposition of residual undecomposed nitrate species in hydrogen [26,27]. The second group of peaks situated between 603 K and 1053 K is mainly attributed to the reduction of CoO particles to

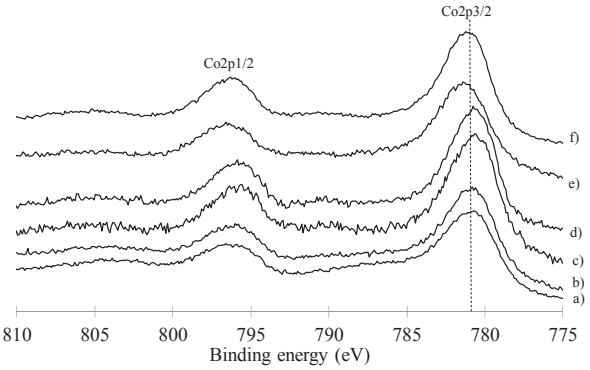

Fig. 5. Co2p XPS spectra of calcined catalysts: a) $10Co/Al_2O_3$, b) $10Co5La/Al_2O_3$, c) $10Co10La/Al_2O_3$, d) co-$10Co10La/Al_2O_3$, e) $10Co15La/Al_2O_3$, and f) $10Co20La/Al_2O_3$.

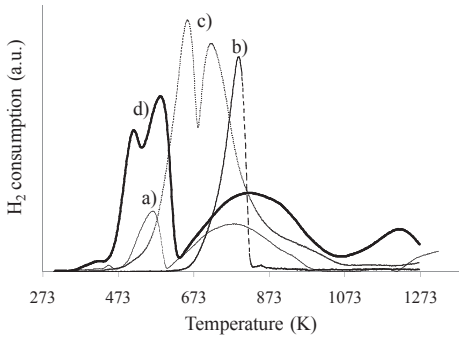

Fig. 6. H_2-TPR profiles of calcined catalysts: a) $10Co/Al_2O_3$, b) $10La/Al_2O_3$, c) $10Co10La/Al_2O_3$, and d) co-$10Co10La/Al_2O_3$.

metallic cobalt and cobalt species interacting strongly with the support, while the high temperature peaks ($T > 1053$ K) could probably be attributed to the reduction of cobalt aluminate compounds and/or very small cobalt oxide particles. The cobalt aluminate compounds are due to the strong interaction between Co_3O_4 and support and can be formed by the introduction of Co(II) in the tetrahedral vacancies of the defect spinel structure of alumina. Table 5 presents the fraction of cobalt in the three domains ($T < 603$ K, $603K < T < 1053$ K and $T > 1053$ K) obtained from the decomposition of the TPR profiles.

The TPR profile of $10La/Al_2O_3$ exhibits a peak at around 773 K, which is attributed to the decomposition of

Table 4
XPS results for $10CoxLa/Al_2O_3$ calcined supported catalysts.

Catalyst	B.E. ($La3d_{5/2}$) (eV)	B.E. (Co $3p_{3/2}$) (eV)	Co/Al Atomic ratio from XPS	La/Al Atomic ratio from XPS	La/Al XPS/bulk	C/Al Atomic ratio from XPS
$10Co/Al_2O_3$	–	780.6	0.03	–	–	–
$10Co5La/Al_2O_3$	835.5	780.7	0.10	0.04	1.9	0.01
$10Co10La/Al_2O_3$	835.5	780.6	0.09	0.12	3	0.03
co-$10Co10La/Al_2O_3$	835.1	780.8	0.08	0.08	2	0.16
$10Co15La/Al_2O_3$	835.9	781.2	0.13	0.27	4.7	0.09
$10Co20La/Al_2O_3$	835.6	781.4	0.44	0.43	5.7	0.21

Co/Al Atomic ratio from bulk = 0.096.

lanthanum carbonates. Note that lanthanum La^{3+} is not reducible at these temperatures (673 K). The TPR profile of the co-10Co10La/Al_2O_3 catalyst obtained by co-impregnation of Co and La is similar to 10Co/Al_2O_3 and exhibits high temperature peaks indicating that co-impregnation is not efficient and does not prevent from the formation of cobalt aluminates. On the other hand, the TPR profile of the 10Co10La/Al_2O_3 catalyst obtained by successive impregnations is very different. The reduction of Co_3O_4 to CoO appears at higher temperatures when lanthanum is present but no cobalt aluminates are observed after 1073 K. This result shows that promotion with 10 wt% of lanthanum allows preventing the formation of the most refractory cobalt aluminate which is responsible for activity loss (Table 5). Fig. 7 presents TPR profiles as a function of lanthanum content. The TPR profiles of 10Co15La/Al_2O_3 and 10Co20La/Al_2O_3 are similar to the profile obtained for the catalyst prepared without lanthanum. The fraction of barely reducible cobalt is similar (around 25%) and close to that of 10Co/Al_2O_3. The value obtained for the 10Co/Al_2O_3 catalyst is in agreement with the literature [28]. This result shows that 10 wt% seems to be the best value for the preparation, in agreement with the limit of good dispersion mentioned above. It seems that the high quantity of lanthanum deposited (>15%) does not allow us to obtain good dispersion of lanthanum and also protection of the support. This suggestion is in agreement with the TPR results showing that the profiles of the catalysts promoted with higher amounts of lanthanum are rather similar to that of the cobalt monometallic catalyst. One of the explanations of the observed phenomena can be deposition of lanthanum species in a tower model rather than in a monolayer.

3.2.2. Catalytic tests

The Fischer–Tropsch catalytic tests were performed on the reference catalyst and the cobalt-lanthanum catalyst containing 10 wt% of La. Indeed we have seen that impregnation of 10 wt% of lanthanum before cobalt introduction allows preventing the formation of the most refractory cobalt aluminate which is responsible for activity loss. Moreover we have seen using XRD that the Co_3O_4 average crystallite size is near the optimum size, and by using XPS that cobalt is well-dispersed as a monolayer. The Fig. 8 presents the catalytic results obtained in terms of conversion and selectivities. CO conversion, methane and higher hydrocarbon selectivity (denoted as S(CH_4) and S(C_{5+})) were determined with time-on-stream at 493 K and 20 bar with a H_2/CO ratio equal to 2. The catalytic

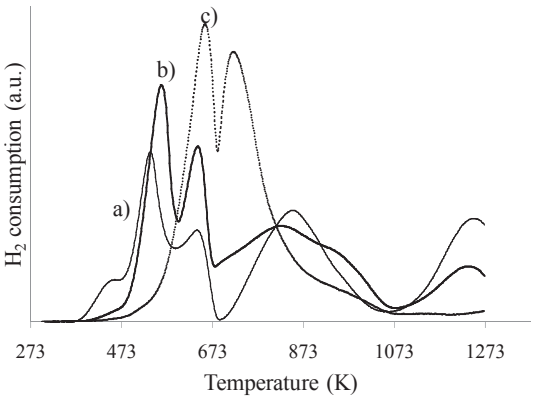

Fig. 7. H_2-TPR profiles of calcined catalysts: a) 10Co20La/Al_2O_3, b) 10Co15La/Al_2O_3, and c) 10Co10La/Al_2O_3.

performance of the monometallic cobalt catalyst was consistent with the available literature data [29–31]. At the beginning of the reaction, conversion obtained with the 10Co10La/Al_2O_3 catalyst is similar to that of 10Co/Al_2O_3. No increase in conversion is observed but the coverage of the support with lanthanum layers allows us to obtain a very low selectivity in methane (3% instead of 10% after 48 h for 10Co/Al_2O_3), which improves catalytic performances. Moreover a higher selectivity of C_{5+} is obtained and no CO_2 was observed. Indeed the selectivity of C_{5+} increases from 83% to 91%, for a time-on-stream of 48 h, when lanthanum is deposited before cobalt introduction. The selectivity of C_2–C_4 hydrocarbons is not affected by the catalyst preparation (around 6%–7% for 10Co10La/Al_2O_3 and 10Co/Al_2O_3 catalysts). Nevertheless cobalt-lanthanum catalysts should be optimized due to their higher deactivation which is observed after several hours when compared with cobalt catalysts. There are various possible mechanisms explaining this deactivation. During the Fischer–Tropsch reaction, cobalt nanoparticles may agglomerate and this will result in the loss of the active surface area [32,33]. This process may be facilitated by the presence of carbonate species. Moreover it has been previously reported that inert carbon phases can form and cause blocking of the active phase [34].

4. Conclusion

The deposition of lanthanum layers on an alumina support was studied. A combination of characterization experiments allowed us to obtain better understanding of

Table 5
Characterization of calcined supported catalysts by TPR.

Catalyst	Fraction of cobalt at low T peaks (298 K < T < 603 K)	Fraction of cobalt at medium T peaks (603 K < T < 1053 K)	Fraction of barely reducible cobalt (T > 1053 K)
10Co/Al_2O_3	31	46	23
10Co5La/Al_2O_3	37	45	18
10Co10La/Al_2O_3	[a]	[a]	0
co-10Co10La/Al_2O_3	49	41	10
10Co15La/Al_2O_3	32	44	24
10Co20La/Al_2O_3	39	35	26

[a] The shape of the curve is different.

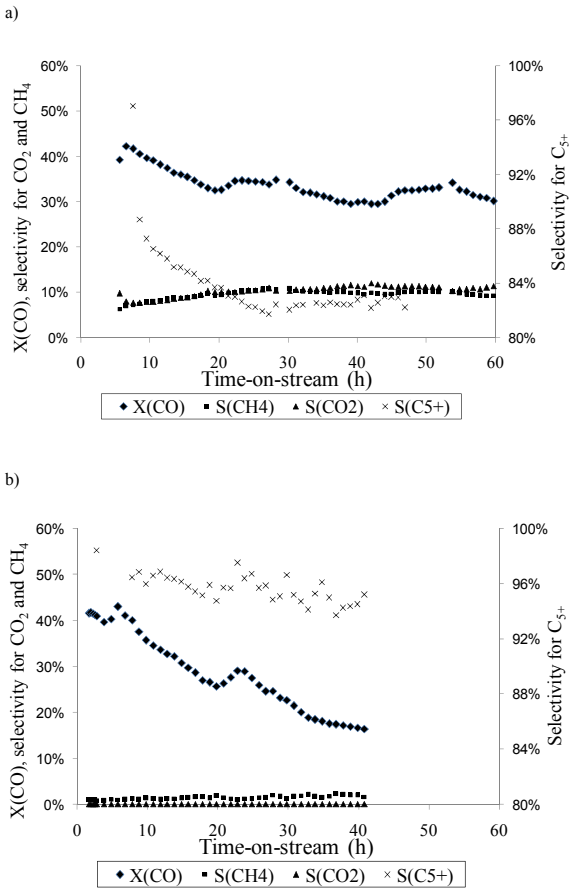

Fig. 8. Variation of CO conversion, methane selectivity $S(CH_4)$, CO_2 selectivity $S(CO_2)$ and C_{5+} selectivity $S(C_{5+})$ with time-on-stream ($T = 220$ °C, $P = 20$ bar, $H_2/CO = 2$, GHSV = 5.6 NL h^{-1} g^{-1}): a) 10Co/Al_2O_3, b) 10Co10La/Al_2O_3.

the interaction between cobalt, lanthanum and alumina in these catalysts. Indeed the results have shown that impregnation of the support with 10 wt% of lanthanum minimizes the concentration of barely reducible cobalt aluminate which is present in conventional cobalt catalysts used for the FT reaction and also to maximize the cobalt metal dispersion. For similar conversion, lower selectivity in methane, and at the same time higher selectivity of heavy hydrocarbons are obtained.

Acknowledgments

The Fonds Européen de Développement Régional (FEDER), CNRS, Région Nord-Pas de Calais and Ministère de l'Éducation Nationale de l'Enseignement Supérieur et de la Recherche are acknowledged for funding of X-ray diffractometers and XPS/LEIS/ToF-SIMS spectrometers within the Pôle Régional d'Analyse de Surface. The authors are grateful in particular to O. Gardoll for the TPR analyses, A.-S. Mamede and M. Trentesaux for XPS analysis and L. Burylo for XRD measurements (Lille-1 University, France).

References

[1] R.B. Anderson, The Fischer–Tropsch Synthesis, Academic Press, New York, 1984.
[2] P. Chaumette, Rev. IFP 51 (1996) 711.
[3] A.C. Vosloo, Fuel Process. Technol. 71 (2001) 149.
[4] A.Y. Khodakov, W. Chu, P. Fongarland, Chem. Rev. 107 (2007) 1692.
[5] M.E. Dry, Catal. Today 71 (2002) 227.
[6] E. Iglesia, S.C. Reyes, R.J. Madon, S.L. Soled, Adv. Catal. 39 (1993) 221.
[7] E. Iglesia, Appl. Catal. A 161 (1997) 59.
[8] G. Jacobs, T.K. Das, Y.Q. Zhang, J.L. Li, G. Racoillet, B.H. Davis, Appl. Catal. A 233 (2002) 263.
[9] E. Iglesia, S.L. Soled, R.A. Fiato, G.H. Via, J. Catal. 143 (1993) 345.
[10] S. Vada, B. Chen, J.G. Goodwin, J. Catal. 153 (1995) 224.
[11] J.S. Ledford, M. Houalls, A. Proctor, D.M. Hercules, J. Phys. Chem. 93 (1989) 6770.
[12] J. Barrault, A. Guilleminot, J.C. Achard, V. Paul-Boncour, A. Percheron-Guegan, Appl. Catal. A 21 (2) (1986) 307.
[13] G.J. Haddad, B. Chen Jr., J.G. Goodwin, J. Catal. 161 (1) (1996) 274.
[14] Ernst, B.; Kiennemann, A.; Chaumette, P. From Book of Abstracts, 213th ACS National Meeting, San Francisco, April 13–17 (1997), FUEL-097.
[15] Y. Zhang, K. Liew, J. Li et, X. Zhan, Catal. Lett. 139 (2010) 1.
[16] Z. Cai, J. Li, K. Liew et, J. Hu, J. Mol. Cat. A: Chem. 330 (2010) 10.
[17] B.D. Cullity, Elements of X-ray Diffraction, Addision-Wesley, London, 1978.
[18] M.F. Sunding, K. Hadidi, S. Diplas, O.M. Lovvik, T.E. Norby, A.E. Gunnaes, J. Electron Spectrosc. Relat. Phenom. 184 (2011) 399.
[19] C.D. Wagner, L.E. Davis, M.V. Zeller, J.A. Taylor, R.H. Raymond, L.H. Gale, Surf. Interface Anal. 3 (1981) 211.
[20] A.Y. Khodakov, R. Bechara, A. Griboval-Constant, Appl. Catal. A 254 (2003) 273.
[21] J.P. Bonnelle, J. Grimblot, A. D'huysser, J. Electron Spectrosc. 7 (1975) 151.
[22] M. Oku, Y. Sato, Appl. Surf. Sci. 55 (1992) 37.
[23] D.G. Castner, P.R. Watson, I.Y. Chan, J. Phys. Chem. 93 (1989) 3188.
[24] V.M. Jiménez, A. Fernández, J.P. Espinós, A.R. González-Elipe, J. Electron Spectrosc. Relat. Phenom. 71 (1995) 61.
[25] A.Y. Khodakov, J. Lynch, D. Bazin, B. Rebours, N. Zanier, B. Moisson, P. Chaumette, J. Catal. 168 (1997) 16.
[26] B. Ernst, A. Bensaddik, L. Hilaire, P. Chaumette, A. Kiennemann, Catal. Today 39 (1998) 329.
[27] A. Jean-Marie, A. Griboval-Constant, A.Y. Khodakov, F. Diehl, Catal. Today 171 (1) (2011) 180.
[28] A. Jean-Marie, A. Griboval-Constant, A.Y. Khodakov, E. Monflier, F. Diehl, Chem. Commun. 47 (2011) 10767.
[29] R. Oukaci, A.H. Singleton, J.G. Goodwin, Appl. Catal. 186 (1999) 129.
[30] P.J. Van Berge, J. Van de Loosdrecht, J.L. Visagie, International Patent WO 01/39882 A1, assigned to Sasol, 7 June 2001.
[31] O. Borg, S. Erib, E.A. Blekkan, S. Storsaeter, H. Wigum, E. Rytter, A. Holmen, J. Catal. 248 (2007) 89.
[32] G.Z. Bian, N. Fujishita, T. Mochizuki, W.S. Ning, M. Yamada, Appl. Catal. A 252 (2003) 251.
[33] M.J. Overett, B. Breedt, E. du Plessis, W. Erasmus, J. van de Loosdrecht, Prepr. Pap.-Am. Chem. Soc., Div. Pet. Chem. 53 (2008) 126.
[34] J.J.H.M. Font Freide, T.D. Gamlin, R.J. Hensman, B. Nay, C. Sharp, J. Nat. Gas Chem. 13 (2004) 1.